

# Superior Therapeutic Index in Lymphoma Therapy: CD30<sup>+</sup> CD34<sup>+</sup> Hematopoietic Stem Cells Resist a Chimeric Antigen Receptor T-cell Attack

Andreas A Hombach<sup>1</sup>, André Görgens<sup>2</sup>, Markus Chmielewski<sup>1</sup>, Florian Murke<sup>2</sup>, Janine Kimpel<sup>3</sup>, Bernd Giebel<sup>2</sup> and Hinrich Abken<sup>1</sup>

<sup>1</sup>Center for Molecular Medicine Cologne, University of Cologne, and Department I for Internal Medicine, University Hospital Cologne, Cologne, Germany; <sup>2</sup>Institute for Transfusion Medicine, University Hospital Essen, University of Duisburg-Essen, Essen, Germany; <sup>3</sup>Division of Virology, Medical University of Innsbruck, Innsbruck, Austria

Recent clinical trials with chimeric antigen receptor (CAR) redirected T cells targeting CD19 revealed particular efficacy in the treatment of leukemia/lymphoma, however, were accompanied by a lasting depletion of healthy B cells. We here explored CD30 as an alternative target, which is validated in lymphoma therapy and expressed by a broad variety of Hodgkin's and non-Hodgkin's lymphomas. As a safety concern, however, CD30 is also expressed by lymphocytes and hematopoietic stem and progenitor cells (HSPCs) during activation. We revealed that HRS3scFv-derived CAR T cells are superior since they were not blocked by soluble CD30 and did not attack CD30<sup>+</sup> HSPCs while eliminating CD30<sup>+</sup> lymphoma cells. Consequently, normal hemato- and lymphopoiesis was not affected in the long-term in the humanized mouse; the number of blood B and T cells remained unchanged. We provide evidence that the CD30<sup>+</sup> HSPCs are protected against a CAR T-cell attack by substantially lower CD30 levels than lymphoma cells and higher levels of the granzyme B inactivating SP6/PI9 serine protease, which furthermore increased upon activation. Taken together, adoptive cell therapy with anti-CD30 CAR T cells displays a superior therapeutic index in the treatment of CD30<sup>+</sup> malignancies leaving healthy activated lymphocytes and HSPCs unaffected.

Received 11 September 2015; accepted 16 March 2016; advance online publication 28 June 2016. doi:10.1038/mt.2016.82

## INTRODUCTION

Adoptive T-cell therapy redirected toward defined targets became one of the most promising strategies in the immunotherapy of cancer during the last years. T cells were equipped with pre-defined target specificity by engineering with a chimeric antigen receptor (CAR), which is composed of an antibody-derived binding domain linked to an intracellular signaling domain for T-cell activation upon target encounter. While adoptive therapy with anti-CD19 CAR-modified T cells produced lasting regression of leukemia/lymphoma,<sup>1,2</sup> the therapy was associated with a lasting B-cell depletion with the need of life-long immunoglobulin

substitution; the identification of a more suitable target for an antitumor attack while preserving healthy tissues remains a major issue. With the rare exceptions of tumor-associated neo-antigens, most potential targets are also expressed by healthy tissues, some of them by somatic stem and progenitor cells; targeting those healthy stem cells may result in an impaired tissue regeneration and serious organ damage in the long-term providing a need to explore the potential targets with respect to targeting the respective stem cells.

CD30 is a prominent example of such a target which is expressed by malignant lymphoid cells, including B- and T-cell leukemia cells and Reed-Sternberg cells of Hodgkin's lymphoma, while also expressed by healthy lymphocytes, although during a small window of antigen-driven maturation.<sup>3,4</sup> Due to the homogeneous and high expression by malignant cells, CD30 is an attractive and validated target for antibody-based therapies,<sup>5</sup> which were proven to be safe. Engineered CAR T cells targeting CD30 have also shown a potent antilymphoma activity in various models,<sup>6–8</sup> however, may cause severe side effects by sustained targeting healthy lymphocytes and, moreover, by targeting hematopoietic stem and progenitor cells (HSPCs), which express CD30 upon cytokine stimulation as revealed by our recent analyses.<sup>9</sup> In this scenario in particular, unintended elimination of HSPCs upon treatment with anti-CD30 CAR T cells would result in a lasting blood cell aplasia.

To explore the risk of targeting CD30 by adoptive T-cell therapy, we monitored in a comparative fashion the CD30 levels in freshly harvested and in cytokine stimulated HSPCs. We recorded *in vitro* and in the humanized Rag2<sup>-/-</sup> cγ<sup>-/-</sup> mouse the cytotoxic potential of anti-CD30 CAR T cells against CD30<sup>+</sup> healthy HSPCs compared with their activity against lymphoma cells. The tested CD30<sup>+</sup> lymphoma cells were efficiently eliminated by anti-CD30 CAR T cells, whereas, the CD30<sup>+</sup> HSPCs were barely affected and retained their full differentiation capabilities and their multilineage reconstitution potential in reconstituted mice, even in the presence of CD30<sup>+</sup> CAR T-cells. The resistance of CD30<sup>+</sup> HSPCs toward the anti-CD30 CAR T cell attack was associated with their substantially lower level of CD30 and the high levels of the granzyme B-inactivating SP6/PI-9 serine protease. The analysis revealed the favorable therapeutic index of the anti-CD30 CAR

Correspondence: Hinrich Abken, Center for Molecular Medicine Cologne, University of Cologne, Robert-Koch-Str. 21, D-50931 Cologne, Germany. E-mail: hinrich.abken@uk-koeln.de

T-cell therapy for the treatment of lymphoma/leukemia in order to eliminate the CD30<sup>+</sup> malignant cells while leaving the healthy CD30<sup>+</sup> HSPCs unaffected.

## RESULTS

### Anti-CD30 CAR T cells mediate a specific response against CD30<sup>+</sup> lymphoma cells and are not blocked by soluble CD30

For the targeted elimination of CD30<sup>+</sup> lymphoma cells, we engineered peripheral blood T cells with the anti-CD30 CAR HRS3scFv-Fc-CD28- $\zeta$ . The CAR is composed in the extracellular moiety of the HRS3 scFv domain for targeting CD30, a mutated IgG1-hinge domain with reduced Fc receptor binding capacities to avoid unintended off-target activation by Fc receptor binding<sup>10</sup> and the intracellular composite CD28 $\Delta$ lck-CD3 $\zeta$  domain for costimulation enhanced CD3 $\zeta$  signaling without the induction of IL-2<sup>11</sup>. Upon retroviral transduction, the anti-CD30 CAR was efficiently expressed on the cell surface of T cells. Anti-CD30 CAR engineered T-cells lysed CD30<sup>+</sup> MyLa cutaneous T lymphoma cells in a dose-dependent manner while coincubated CD30<sup>-</sup> Colo320 tumor cells were not affected (Figure 1a). Anti-CD30 CAR-mediated T-cell activation was not restricted toward T lymphoma cells since CD30<sup>+</sup> L1236 Hodgkin's B lymphoma cells were also eliminated with similar efficiency (Figure 1b). Following subcutaneous coinjection of CD30<sup>+</sup> MyLa cells into immune-deficient mice, CAR T cells suppressed the establishment of cutaneous lymphoma in a dose-dependent manner (Figure 1c). Thus, anti-CD30 CAR T cells specifically attack CD30<sup>+</sup> lymphoma cells. CD30 is shedded by CD30<sup>+</sup> lymphoma cells and increased serum CD30 levels accompany progression of CD30<sup>+</sup> lymphoma/leukemia.<sup>12</sup> Cell activation by HRS3scFv containing CARs, however, is not blocked *in vitro* by soluble CD30 in concentrations which are higher as usually observed in lymphoma patient (Figure 1d). Notably, blocking of the HRS3scFv-CAR by the anti-idiotypic mAb 9G10 resulted in dose-dependent inhibition of cellular activation indicating different kinetics. We therefore conclude that the anti-CD30 CAR HRS3scFv-Fc-CD28- $\zeta$  is a favorite CAR to redirect T cells toward lymphoma/leukemia.

### CD30 is expressed by all HPSC subsets

We previously reported that cytokine stimulation induces CD30 expression on a subset of human umbilical cord blood (UCB)-derived CD34<sup>+</sup> cells.<sup>9</sup> CD30 is furthermore expressed by a subset of activated T and B cells.<sup>13</sup> With respect to safety, HSPCs are a crucial cell compartment and must not be targeted to maintain hematopoiesis upon CD30 redirected CAR T-cell therapy. Therefore, we assessed whether CD30<sup>+</sup> HSPCs are recognized and eliminated by anti-CD30 CAR T cells. At first, we studied CD30 cell surface expression of freshly isolated and of cytokine stimulated CD34<sup>+</sup> cells. While only few CD34<sup>+</sup> cells in the freshly isolated population expressed CD30 (Figure 2a, day 0), CD30 was upregulated upon cytokine stimulation, peaking to more than 60% CD30<sup>+</sup> cells on days 2 and 3 of culture (Figure 2a,b).

Since CD34<sup>+</sup> cells comprise a heterogeneous pool of primitive hematopoietic cells, we asked whether CD30 expression may be associated to lineage commitment. We subfractionated HSPCs according to CD133, CD45RA, CD38, and CD10 expression by

HSC/multipotent hematopoietic progenitors (HSC/MPP), lymphoid-primed multipotent (LMPP), granulocyte and macrophage primed (GMP), multi-lymphoid primed, and common erythromyeloid primed progenitors (Figure 2c); the details for the identification of the subsets are summarized in Supplementary Figure S1.<sup>14,15</sup> We addressed by multicolor flow-cytometric analyses whether transient CD30 expression is specifically associated with lineage commitment. In three independent experiments, freshly isolated CD34<sup>+</sup> cells were either immediately characterized (day 0) or upon cultivation in the presence of cytokines. Cells with weak CD30 cell surface expression were found in all subsets at day 0, with the highest numbers in the LMPP and GMP and the lowest numbers in the HSC/MPP fraction (Figure 2d). Due to the induction by serum and cytokines, the CD38 expression strength does not discriminate LMPP from GMP cells and both progenitor cell types were cultured together (Figure 2d). CD30 was detected on cells of all HSPC subsets, with the highest number of CD30<sup>+</sup> cells within the LMPP and multi-lymphoid primed subsets and with 1 day delay in the MPP subset. Thus, CD30 expression is rather associated with the HSPC maturation but less with a certain HSPC subtype.

### Anti-CD30 CAR T cells did not eliminate activated CD30<sup>+</sup> HSPCs

To assess whether the CD30<sup>+</sup> HSPCs are potential targets for an anti-CD30 CAR T-cell attack, HSPCs were coincubated with flow-sorted CAR T cells (Figure 3a). As controls, HSPCs were cultured with T cells lacking the CAR or MyLa lymphoma cells were used as alternative target cells. Whereas the CD30<sup>+</sup> MyLa cells were killed by the anti-CD30 CAR T cells, the HSPC population was not reduced (Figure 3b,c). To detect specific cytolysis against the CD30<sup>+</sup> HPSC subset, we sorted HSPCs into the CD30<sup>-</sup> and CD30<sup>+</sup> cells (Figure 4a) and coincubated these cells with flow-sorted T cells with and without CAR, respectively. As summarized in Figure 4b, CAR T cells produced slightly enhanced killing of CD30<sup>+</sup> HSPCs compared to CD30<sup>-</sup> HSPCs; however, cytolysis was substantially less efficient than lysis of the MyLa lymphoma cells in the same preparation.

### Anti-CD30 CAR T cells did not affect lymphocyte or myeloid cell differentiation

We investigated whether anti-CD30 CAR T cells may impact the maturation capabilities of cocultured HSPCs. As demonstrated in Figure 5a, coculture with anti-CD30 CAR T cells did not affect myeloid colony formation of the HSPCs, but slightly decreased their potential in erythroid colony formation. To test for adverse effects of the CAR T cells *in vivo*, Rag2<sup>-/-</sup>  $\gamma$ <sup>-/-</sup> mice were transplanted with HSPCs to establish human hematopoiesis. Upon successful engraftment, autologous T cells with engineered anti-CD30 CAR or anti-carcinoembryonic antigen (CEA) CAR for control were adoptively transferred. To reveal their impact on the human hematopoiesis, the number of human peripheral blood T or B cells was monitored over 50 days. The number of CD3<sup>+</sup> T cells and CD19<sup>+</sup> B cells was not altered in any mouse treated with CAR T cells and not in the control mice which received T cells with an anti-CEA CAR (Figure 5b). Of note, adoptively transferred anti-CD30 CAR T cells persisted in the blood and in multiple organs of

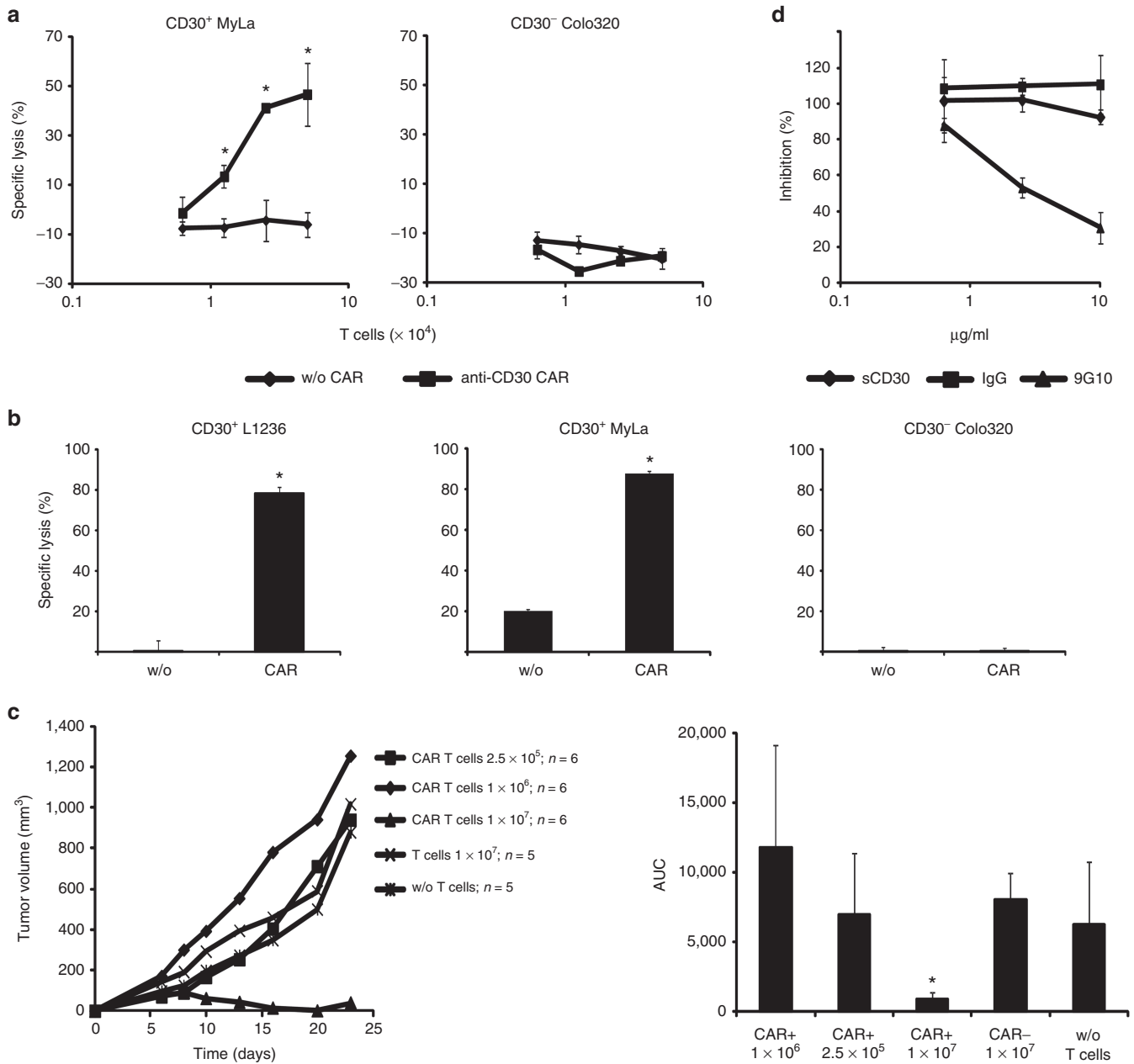


**Figure 1** Anti-CD30 chimeric antigen receptor (CAR) T cells mediate a specific response against CD30<sup>+</sup> lymphoma cells *in vitro* and *in vivo*. Anti-CD30 CAR T cells lyse CD30<sup>+</sup> lymphoma cells of different origin in a dose-dependent manner. **(a)** T cells from the peripheral blood were engineered with the anti-CD30 CAR and cocultivated in serial dilutions ( $0.5\text{--}5 \times 10^4/\text{well}$ ) with CD30<sup>+</sup> MyLa cutaneous T lymphoma cells or CD30<sup>-</sup> Colo320 tumor cells ( $5 \times 10^4/\text{well}$ ) for 48 hours in 96-well round bottom plates. Coincubation of lymphoma cells with T cells without CAR (w/o CAR) served as control. The assay was done in triplicates and mean values  $\pm$  standard deviation (SD) were determined. Data represent mean values of one representative out of three experiments. **(b)** CAR T cells ( $2.5 \times 10^4/\text{well}$ ) were cocultivated with CD30<sup>+</sup> MyLa, L1236 Hodgkin's lymphoma cells, and CD30<sup>-</sup> Colo320 tumor cells (each  $5 \times 10^4/\text{well}$ ), respectively. T cells without CAR (w/o) served as control. Specific lysis of tumor cells was determined by an XTT-based assay. The assay was done in triplicates and mean values ( $\pm$ SD) were determined. Data represent mean values of one representative out of five experiments. *P* values were calculated by Student's *T*-test. Asterisks indicate significant differences between groups (*P* < 0.05). **(c)** Anti-CD30 CAR T cells suppress tumor growth *in vivo* in a dose-dependent fashion. CAR T cells ( $2.5 \times 10^5\text{--}1 \times 10^7$  cells/mouse) were coinjected with MyLa cutaneous T lymphoma cells ( $10^7/\text{mouse}$ , groups of five or six animals) and tumor growth was monitored every 2–3 days. Mean values of the tumor volume (left) and the area under curve values (right) ( $\pm$ SD) were determined. *P* values were calculated by Student's *T*-test. Asterisks indicate significant differences (*P* < 0.05) compared with the control group. **(d)** Blocking of CAR T cells by soluble CD30-Fc. MD45 T cells with anti-CD30 CAR were cocultivated with CD30<sup>+</sup> L540cy cells (each  $5 \times 10^4/\text{well}$ ) in presence of increasing amounts of CD30-Fc, the HRS3-specific anti-idiotypic mAb 9G10 and an isotype control mAb, respectively. After 48 hours, culture supernatants were removed, analyzed for IL-2 secretion and blocking of CAR T-cell inhibition was determined as described in Materials and Methods. The assay was done in triplicate samples and the mean values  $\pm$  SD were determined.

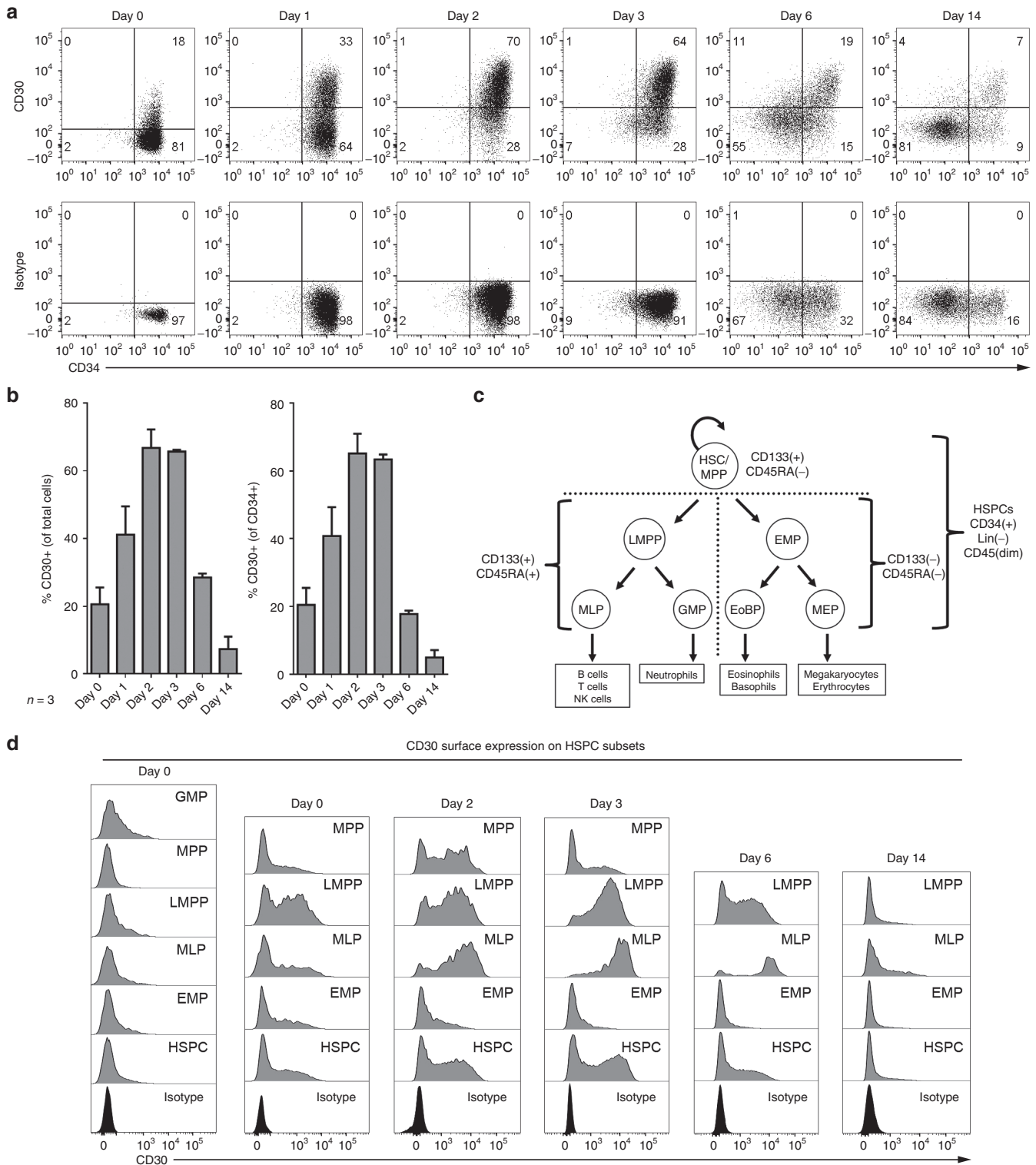


**Figure 2** CD34<sup>+</sup> hematopoietic stem and progenitor cells (HSPCs) express CD30 upon activation and differentiation. **(a)** CD30 surface expression on freshly isolated (day 0) and cultured CD34<sup>+</sup> cells. **(b)** Quantification of CD30 on the cell surface over time based on flow-cytometric data (as shown in **a**) of umbilical cord blood derived CD34<sup>+</sup> cells from three donors, presented as relative values of all cells or of CD34<sup>+</sup> cells (± SD). **(c)** Human hematopoietic tree and definition of HSPC subsets. **(d)** CD30 expression on HSPC subsets. We used the following marker combinations to identify fractions enriched for HSCs/MPPs (CD34<sup>+</sup>CD133<sup>+</sup>CD45RA<sup>-</sup>CD38<sup>low</sup>CD10<sup>-</sup>), lymphoid-primed multipotents (LMPPs) (CD34<sup>+</sup>CD133<sup>+</sup>CD45RA<sup>+</sup>CD38<sup>low</sup>CD10<sup>-</sup>), GMPs (CD34<sup>+</sup>CD133<sup>+</sup>CD45RA<sup>+</sup>CD38<sup>+</sup>CD10<sup>-</sup>); multi-lymphoid primed progenitors (CD34<sup>+</sup>CD133<sup>+</sup>CD45RA<sup>+</sup>CD38<sup>low</sup>CD10<sup>+</sup>) and erythro-myeloid primed progenitors (CD34<sup>+</sup>CD133<sup>low</sup>CD45RA<sup>-</sup>).<sup>14</sup> Since the CD38 expression after initiation of culture is not indicative to discriminate LMPP and GMP-enriched fractions, we neglected its expression for HSPC subset gating on cultured samples and pooled LMPP and GMP fractions to an LMPP fraction.<sup>15,36</sup> A dump channel excluding 7-AAD-positive dead cells and lineage (CD3, CD19, CD56, CD66b) positive cells and a CD45<sup>dim</sup> gate were used for all experiments (see **Supplementary Figure S1** for details). The flow-cytometric data show one representative out of three independent analyses; cells from three donors were analyzed.

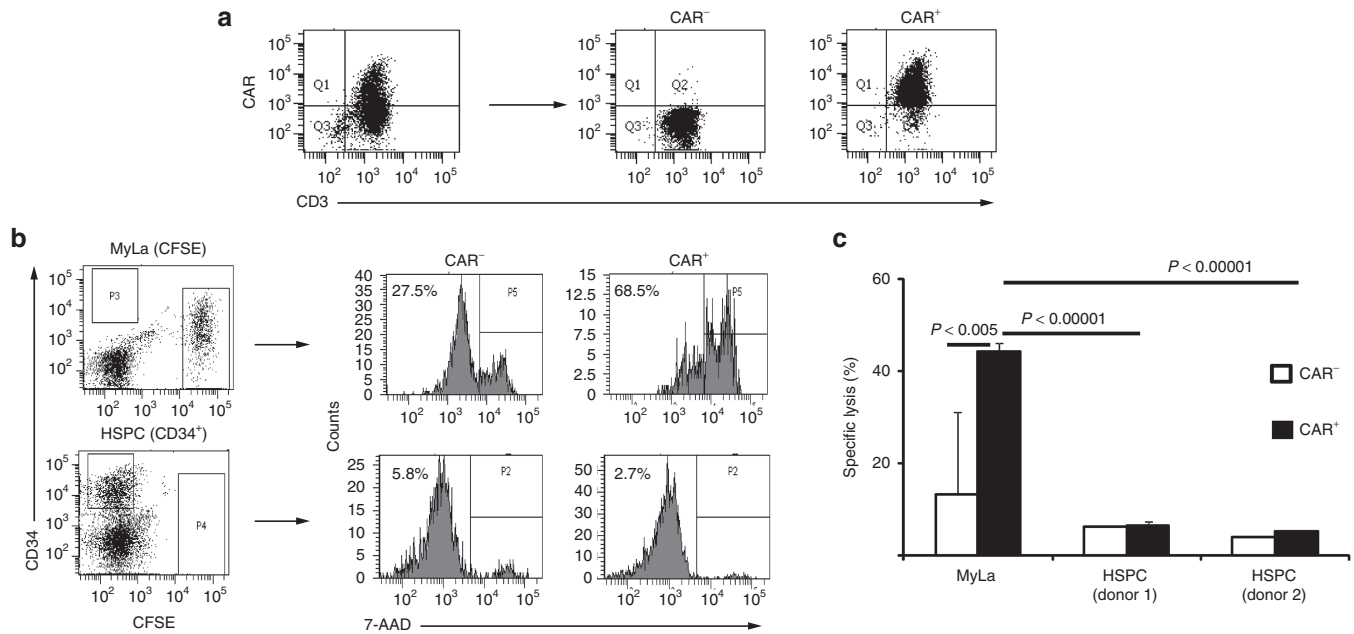


**Figure 3** Anti-CD30 chimeric antigen receptor (CAR) T cells do not lyse activated hematopoietic stem and progenitor cells (HSPCs). **(a)** Flow cytometric cell sorting of CAR<sup>+</sup> and CAR<sup>-</sup> T cells. T cells were engineered with the anti-CD30 CAR, stained with anti-hlgG1 and anti-CD3 antibodies to detect CAR<sup>+</sup> T cells and flow sorted to obtain the CD3<sup>+</sup> CAR<sup>-</sup> and CD3<sup>+</sup> CAR<sup>+</sup> T-cell subsets. **(b,c)** Cocultivation of CAR T cells with HSPCs and CD30<sup>+</sup> lymphoma cells. HSPCs from two healthy donors were isolated by magnetic cell separation procedures from umbilical cord blood and activated in the presence of FLT3L, SCF, and TPO for 72 hours. Carboxyfluorescein diacetate succinimidyl ester (CFSE)-labeled CD30<sup>+</sup> MyLa lymphoma cells ( $2 \times 10^4$  / well) and activated HSPCs  $1 \times 10^4$  (donor UCB612) and  $2 \times 10^4$  cells/well (donor UCB615), were cocultivated for 24 hours each with sorted CAR<sup>-</sup> and CAR<sup>+</sup> T cells ( $2 \times 10^4$ /well), respectively, in 96-well round bottom plates. Cells were recovered and HSPCs labeled with an anti-CD34-PE antibody. Cells were analyzed by flow cytometry and dead cells were identified by 7-AAD staining (0.5  $\mu$ g/ml). Representative dot blots demonstrating the gating strategy of CD34<sup>+</sup> HSPCs and CFSE-labeled MyLa lymphoma cells and histograms of 7-AAD staining indicating target-cell lysis upon cocultivation with CAR T cells are shown **(b)**. 7-AAD staining data were used to calculate specific lysis as described in Materials and Methods **(c)**. The assay was done in triplicates and the mean values  $\pm$  SD were determined. Data show representative results of three analyses with different donors. *P* values were calculated by Student's *T*-test and significant differences between relevant groups are indicated.

the treated mice until the end of the observation period as detected by PCR specific for the genomic integrates of the unique anti-CD30 CAR DNA sequences (**Supplementary Figure S2**). Data indicate that the human hematopoiesis in the humanized Rag2<sup>-/-</sup> c $\gamma$ <sup>-/-</sup> mouse was not substantially affected indicating a robust resistance of HSPCs toward an anti-CD30 CAR T-cell attack.

### CD30<sup>+</sup> HSPCs expressed CD30 below the T-cell activation threshold

There may be at least two, mutually not exclusive mechanisms for the resistance of CD30<sup>+</sup> HSPCs toward a lytic CAR T-cell attack. First, the CD30 level may be below the threshold to elicit a CAR-mediated T-cell response; second, HSPCs may harbor cell-intrinsic protection molecules, which harness these cells against a cytolytic T-cell attack. We compared CD30 expression levels of activated HSPCs of several donors with those of MyLa lymphoma cells by flow cytometry. As demonstrated in **Figure 6a,b**, MyLa tumor cells have a more than four times higher mean fluorescence intensity (mfi) of CD30 staining than the CD30<sup>+</sup> HSPCs.

To address whether the CD30 level on a target cell impacts CAR T cell-mediated cytotoxicity, we took the advantage of MC38 cells, which lack CD30 and which we engineered to express human CD30 at different levels on their cell surface in order to obtain cells with low and high CD30 levels. CD30<sup>+</sup> MC38

cells with different CD30 levels were sorted by flow cytometry (**Figure 6c**) and coincubated with CAR T cells. Specific cytotoxicity and IFN- $\gamma$  secretion indicating T-cell activation were recorded and plotted as a function of the CD30 level of the target-cell surface. As summarized in **Figure 6d**, the CD30 level correlated with the target-cell elimination; however, above a certain CD30 level, further increase did not improve target-cell lysis. On the other hand, CD34<sup>+</sup> HSPCs expressed CD30 levels near the threshold for CAR T-cell activation inducing only background to minor cytolytic activities. Compared to CAR T cell-mediated cytotoxicity, the induction of IFN- $\gamma$  release required much higher CD30 levels on the target cells (**Figure 6e**). We assumed that the CD30 level on HSPCs is near or below the cytolytic activation threshold and are not sufficient to initiate a productive CAR T-cell response with respect to cytolysis and IFN- $\gamma$  release.

Since nonmalignant CD30<sup>+</sup> immune cells, like activated B cells, are also potential target cells,<sup>16</sup> we asked whether these cells express CD30 above the CAR T-cell activation threshold. MACS-isolated B cells were activated by soluble CD40L and IL-4 and separated into CD19<sup>+</sup> CD30<sup>-</sup> or CD19<sup>+</sup> CD30<sup>+</sup> subsets. Flow cytometric analyses revealed CD30 levels on B cells in the range of those of HSPCs (**Figure 6f**). Consequently, we did not record specific lysis of CD30<sup>+</sup> B cells upon coincubation with anti-CD30 CAR T cells whereas CD30<sup>+</sup> MyLa tumor cells for control were lysed with high efficiency (**Figure 6g**).

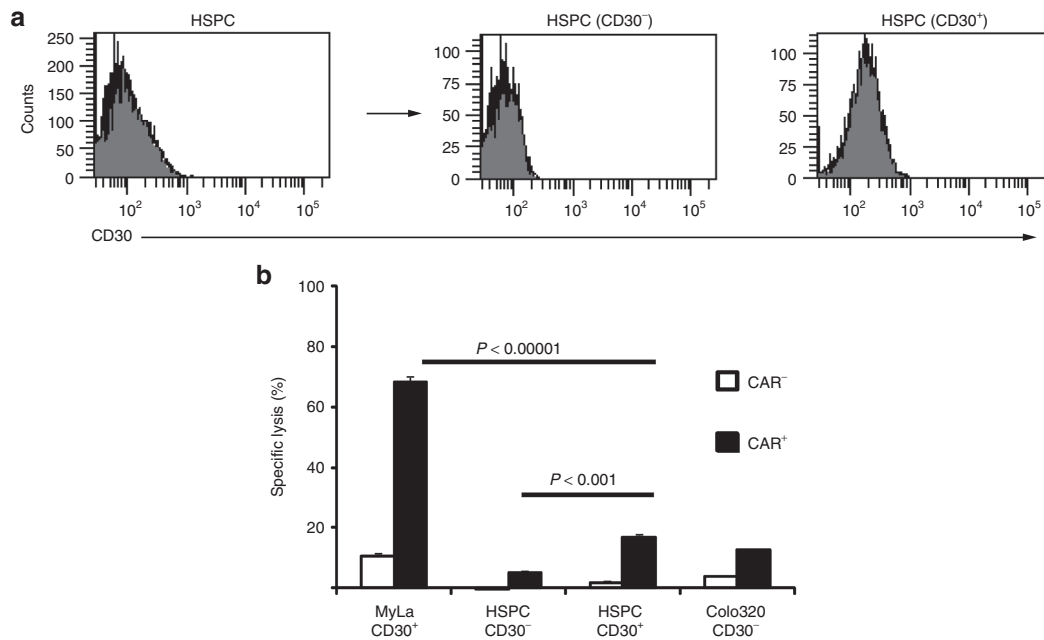


**Figure 4** Anti-CD30 chimeric antigen receptor (CAR) T cells preferentially lyse CD30<sup>+</sup> lymphoma cells but not purified CD30<sup>+</sup> hematopoietic stem and progenitor cell (HSPC). **(a)** CD34<sup>+</sup> HSPCs were isolated by magnetic cell separation from umbilical cord blood of healthy donors, activated for 3 days, stained with anti-CD34-PE and anti-CD30-FITC antibodies and sorted by flow-cytometry into CD30<sup>-</sup> and CD30<sup>+</sup> subsets. **(b)** Anti-CD30 CAR T cells were flow sorted into CAR<sup>+</sup> and CAR<sup>-</sup> subsets and coincubated ( $2 \times 10^4$  cells/well) with carboxyfluorescein diacetate succinimidyl ester-labeled MyLa cells ( $2 \times 10^4$ /well) or with flow-sorted CD30<sup>+</sup> and CD30<sup>-</sup> HSPCs (each  $1 \times 10^4$  cells/well) for 24 hours. Cells were recovered and stained with anti-CD34 antibody and 7-AAD. The numbers of viable and dead cells were determined and specific lysis was calculated as described in Materials and Methods. The assay was done in triplicate samples and mean values  $\pm$  SD of a representative analysis out of three are demonstrated. *P* values were calculated by Student's *T*-test and significant differences between relevant groups are indicated.

### CD30<sup>+</sup> HSPCs did not induce specific degranulation of CAR T cells but express high levels of the granzyme B inhibitor PI-9 and were not affected by bystander-mediated cytotoxicity

We analyzed whether the capability of anti-CD30 CAR T cells to discriminate between CD30<sup>+</sup> lymphoma cells and CD30<sup>+</sup> HSPCs are mirrored by an antigen-specific degranulation of the CAR T cells. To address this issue, we recorded CD107a on the surface of activated anti-CD30 CAR T cells upon contact with CD30<sup>+</sup> target cells. Flow cytometric data confirmed that CAR T cells did not increase cytolytic degranulation upon contact to CD30<sup>+</sup> HSPCs while MyLa cells substantially increased CD107a staining of anti-CD30 CAR T cells (Figure 7a). For comparison, no specific cytolytic degranulation was observed when T cells without CAR were coincubated with the respective target cells. Of note, the spontaneous degranulation of anti-CD30 CAR T cells was substantially higher than of T cells without CAR indicating some CAR intrinsic T-cell activation. In summary, data revealed the insufficiency of CD30<sup>+</sup> HSPCs to induce specific degranulation of cytolytic anti-CD30 CAR T cells.

We now asked whether MyLa lymphoma cells which induce anti-CD30 CAR T-cell activation cause bystander killing of HSPCs by CAR T-cells or, vice versa, HSPCs protect MyLa cells from CAR T-cell killing. To this end, we coincubated anti-CD30 CAR T cells together with both MyLa cells and CD30<sup>+</sup> HSPCs. We identified HSPCs by CD34, MyLa cells by CFSE labeling and recorded the number of dead carboxyfluorescein diacetate succinimidyl ester (CFSE)<sup>+</sup> MyLa cells and CD34<sup>+</sup> HSPCs, respectively,

by flow cytometry in the same assay. As summarized in Figure 7b, MyLa cells were eliminated by CAR<sup>+</sup> T cells with high efficiency while the coincubated CD30<sup>+</sup> HSPCs were not affected. Taken together, we conclude that activated HSPCs were hardly eliminated in a direct or indirect manner by anti-CD30 CAR T cells while CD30<sup>+</sup> lymphoma cells were efficiently eliminated.

Since CD30<sup>+</sup> HSPCs were resistant toward direct cytotoxicity by anti-CD30 CAR T cells due to subthreshold CD30 levels, we addressed whether HSPCs may additionally be protected by a cell intrinsic mechanism. We hypothesized that the granzyme B-inactivating serine protease PI-9 may be involved in this process. Primarily described as a self-protecting mechanism of cytolytic T cells,<sup>17</sup> PI-9 also protects mesenchymal and embryonic stem cells from a T-cell attack.<sup>18-20</sup> We monitored the PI-9 levels in HSPCs in comparison to CD30<sup>+</sup> lymphoma cells by flow cytometry. As summarized in Figure 7c, HSPCs expressed PI-9 at substantially higher levels than healthy lymphocytes and a panel of CD30<sup>+</sup> lymphoma cell lines. Notably, there were no substantial differences in the PI-9 levels of CD30<sup>+</sup> and CD30<sup>-</sup> HSPCs (Figure 7d). While freshly isolated HSPCs had higher PI-9 levels than lymphoma cells, the levels furthermore increased upon cytokine-mediated activation (Figure 7e). Taken together, we conclude that HSPCs are likely protected from a cytolytic anti-CD30 CAR T-cell attack by near-threshold CD30 and high PI-9 levels.

## DISCUSSION

CD30 is a good candidate for redirected T-cell therapy since it is highly expressed by a panel of B and T lymphoma cells but to a far

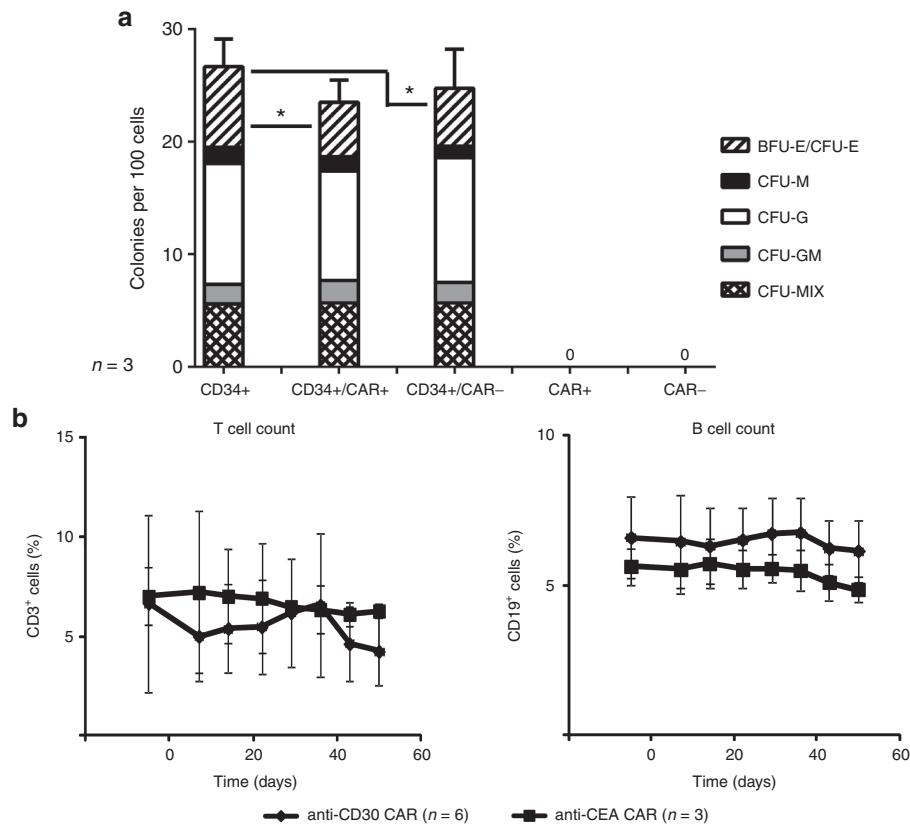


**Figure 5** Anti-CD30 chimeric antigen receptor (CAR) T cells do not affect myeloid and lymphocyte cell differentiation. **(a)** To assay colony-forming capacity, 200 CD34<sup>+</sup> hematopoietic stem and progenitor cells (HSPCs), which had been stimulated for 2 days with FLT3L, SCF, and TPO to induce CD30, were cultured in the presence or absence of CAR<sup>+</sup> or CAR<sup>-</sup> T cells (200/well) in 96-well round-bottom plates. After 24 hours, cells were harvested and seeded in MethoCult H4434 medium to induce erythro-myeloid cell differentiation. Hematopoietic colonies were scored after 12–14 days as described in Materials and Methods. Data of three HSPC donors are shown. **(b)** Newborn Rag2<sup>-/-</sup> cγ<sup>-/-</sup> mice were grafted with human CD34<sup>+</sup> HSPCs (1–3 × 10<sup>5</sup>/mouse). After successful engraftment of human hematopoiesis autologous T cells with or without anti-CD30 or anti-carcinoembryonic antigen (CEA) CAR were transferred into mice at day 0 (2.5 × 10<sup>6</sup> cells/mouse; six mice with anti-CD30 CAR T cells; three mice with anti-CEA CAR T cells). Blood was recovered once per week and B and T cells were identified by flow cytometry upon staining with anti-CD3 and anti-CD19 antibodies, respectively. Data represent mean values ± SD. *P* values were calculated by the Student's *T*-test. Asterisks indicate significant differences between groups (*P* < 0.05).

lesser extent by healthy cells including activated lymphocytes.<sup>5</sup> Our group was the first to engineer a CAR for redirecting T cells specifically toward CD30 for the treatment of B-cell Hodgkin's lymphoma and cutaneous T-cell lymphoma.<sup>6</sup> Currently, anti-CD30 CAR T cells are clinically explored in the adoptive cell therapy of Hodgkin's lymphoma<sup>21</sup>; a trial for the treatment of cutaneous lymphoma is in planning (NCT01645293). Here we revealed that, in addition to activated lymphocytes, cytokine stimulated HSPCs, especially progenitors of the LMPP and MMP subsets, also express CD30 making these cells potential targets of an anti-CD30 CAR T-cell therapy with the risk of a lasting impairment of hematopoiesis and anemia and lymphodepletion in the treated patients. This impairment would be more severe on repopulating CD34<sup>+</sup> cells which are activated upon lymphodepletion usually preceding CAR T-cell therapy. Such disturbance would be more severe and clinically less manageable than a selective B-cell depletion upon anti-CD19 CAR therapy as currently experienced in trials.<sup>1,22,23</sup>

Our comprehensive safety evaluation with this respect revealed that adoptive cell therapy with HRS3scFv-FcΔ-CD28Δ-ζ CAR engineered T cells have a high therapeutic index based on the following properties. The CAR T cells (i) selectively kill

CD30<sup>+</sup> lymphoma cells while there is no substantial direct or indirect cytotoxicity against CD30<sup>+</sup> HSPCs in cocultivation assays, (ii) efficiently eliminate CD30<sup>+</sup> lymphoma cells in a transplantation model, (iii) preserve the erythro-myeloid cell differentiation of cocultured HSPCs, and (iv) preserve an engrafted human hematopoietic system in the reconstituted Rag2<sup>-/-</sup> cγ<sup>-/-</sup> mouse with normal blood lymphocyte counts in the long-term. The data indicate that anti-CD30 CAR T cells display a profound antilymphoma activity while preserving the CD34<sup>+</sup> CD30<sup>+</sup> HSPCs and their differentiation capacity. A caveat is that the anti-CD30 CAR T cells were applied after establishment of the human hematopoietic system in the humanized mouse; lymphodepletion and repopulation of CD34<sup>+</sup> cells with the generation of CD30<sup>+</sup> HSPCs usually occurs immediately before CAR T-cell therapy. The early toxicities on the repopulating hematopoiesis were here only addressed by *in vitro* assays.

Different and likely synergistic mechanisms contribute to the profound resistance of CD30<sup>+</sup> HSPCs toward a cytolytic attack by anti-CD30 CAR T cells. First, the subthreshold level of the targeted CD30 on HSPCs while lymphoma cells express CD30 clearly above the threshold for CAR T-cell activation.

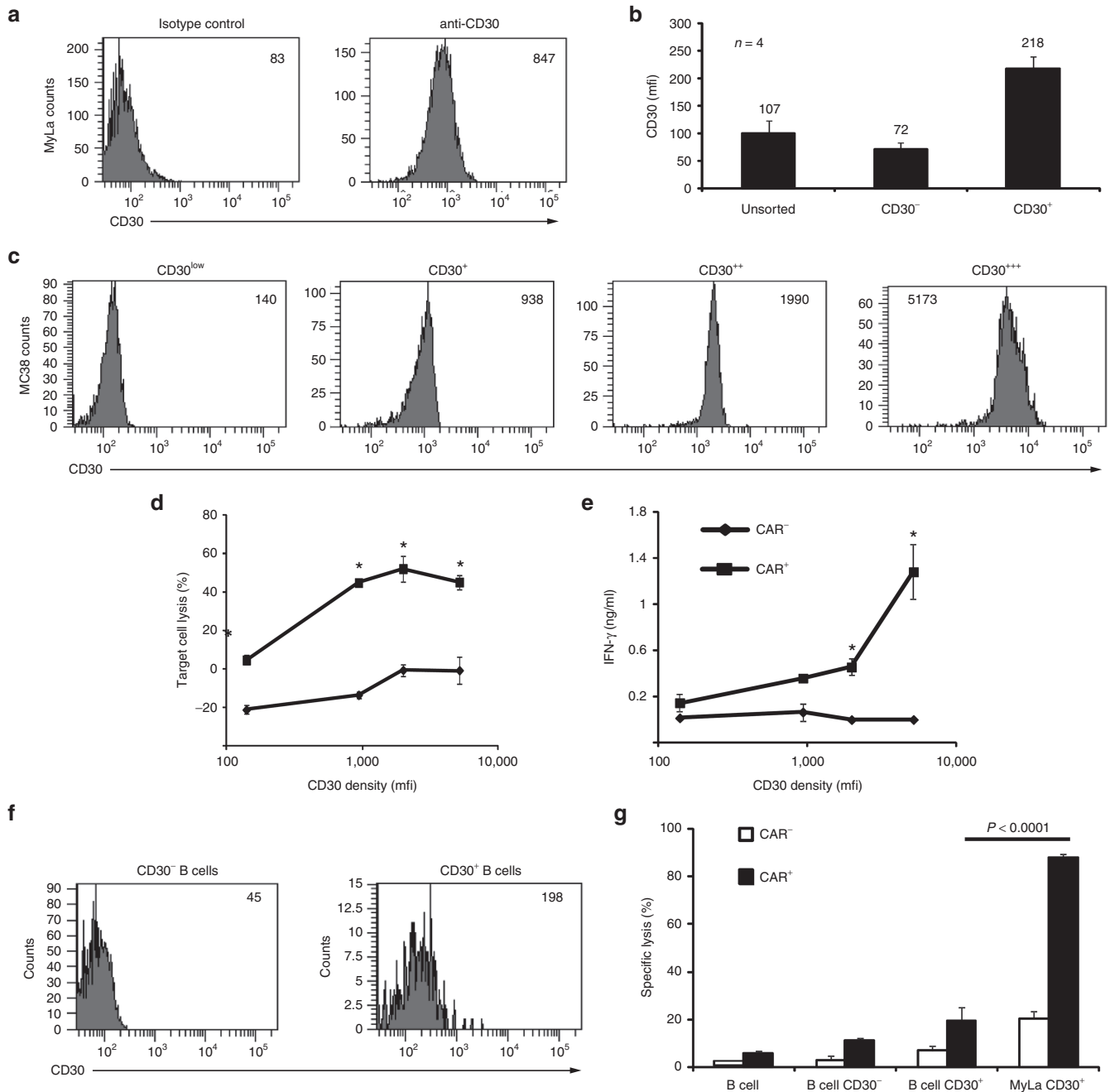


**Figure 6** CD30<sup>+</sup> hematopoietic stem and progenitor cells (HSPCs) and B cells express CD30 below the activation threshold of anti-CD30 chimeric antigen receptor (CAR) T cells. **(a–c)** Comparison of CD30 levels on target cells. **(a)** MyLa lymphoma cells were stained with the anti-CD30 antibody or an isotype control antibody and recorded by flow cytometry. **(b)** HSPCs from four donors were activated and flow sorted into the CD30<sup>-</sup> and CD30<sup>+</sup> subpopulations utilizing the same anti-CD30 antibody; the mean fluorescence intensity (mfi) was recorded. **(c)** Mouse MC38 tumor cells which lack CD30 were engineered to express human CD30. Cells were stained with the anti-CD30 antibody and flow sorted into subsets with different CD30 levels. Numbers in histograms and above columns represent mfi of CD30 staining in arbitrary units. **(d,e)** Sorted MC38 tumor cells ( $2.5 \times 10^4$ /well) were cocultivated for 24 hours with T cells with or without anti-CD30 CAR ( $2.5 \times 10^4$ /well). Target-cell lysis was determined by the XTT-assay **(d)** and IFN- $\gamma$  concentration in the supernatants by ELISA **(e)**. The assay was done in triplicate, mean values  $\pm$  SD determined and plotted against the mfi of CD30 of the respective target-cell subset. *P* values were determined by the Student's *T*-test and significant differences (*P* < 0.05) indicated by asterisks. The assay was performed twice with similar results. **(f)** B cells were activated and flow sorted into CD30<sup>-</sup> and CD30<sup>+</sup> subpopulations utilizing the anti-CD30 mAb as described in Materials and Methods. **(g)** Unseparated and CD30<sup>+</sup> or CD30<sup>-</sup> B cells (each  $1 \times 10^4$ /well) were cocultivated with CAR<sup>+</sup> or CAR<sup>-</sup> T cells ( $2.5 \times 10^4$ /well) for 48 hours. B cells were identified by staining with the anti-CD19 mAb, dead cells by staining with 7-AAD (0.5  $\mu$ g/ml) and the number of dead and live B cells was recorded by flow cytometry. Specific B-cell lysis was calculated as described. For comparison, cytotoxicity of MyLa cells by CAR T cells was tested in parallel. The assay was done in triplicates and mean values  $\pm$  SD were determined. *P* values of relevant groups were determined by the Student's *T*-test. Data of one representative analysis out of two are shown.



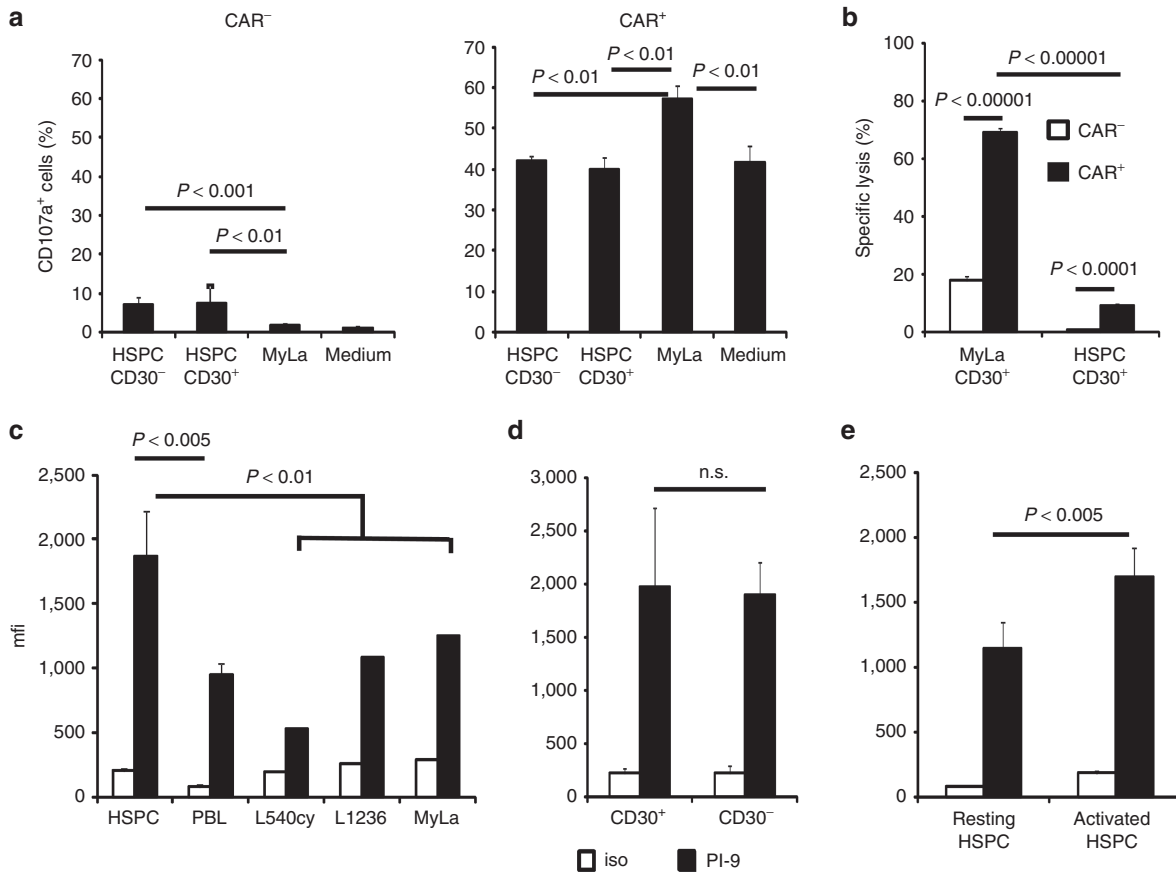


**Figure 7** Hematopoietic stem and progenitor cells (HSPCs) did not induce CD30-specific degranulation of chimeric antigen receptor (CAR) T cells, are protected against bystander lysis and express high levels of the granzyme B inhibitor PI-9. **(a)** CAR T cells specifically degranulate in the presence of CD30<sup>+</sup> lymphoma cells but not CD30<sup>+</sup> HSPC cells. Anti-CD30 CAR T cells ( $4 \times 10^4$  cells/well) were coincubated with CD30<sup>+</sup> MyLa lymphoma cells and flow-sorted CD30<sup>+</sup> or CD30<sup>-</sup> HSPCs (each  $2 \times 10^4$  cells/well), respectively. Degranulating T cells were identified by staining for CD107a. After 12 hours, T cells were recovered, stained additionally with anti-CD3 and anti-human IgG1 antibodies to detect CD3<sup>+</sup> CAR<sup>+</sup> and CD3<sup>+</sup> CAR<sup>-</sup> T cells, respectively, and analyzed by flow cytometry. Mean values  $\pm$  SD of triplicates were determined and p values calculated by the Student's *T*-test. **(b)** HSPC bystander lysis by CAR T cells in the presence of CD30<sup>+</sup> MyLa lymphoma cells. Carboxyfluorescein diacetate succinimidyl ester (CFSE) labeled MyLa cells ( $2 \times 10^4$  cells/well) and CD30<sup>+</sup> HSPCs ( $1 \times 10^4$  cells/well) were together cocultivated with T cells with or without CAR. Cells were harvested, labeled with an anti-CD34 antibody and 7-AAD and the number of viable and dead CD34<sup>+</sup> HSPCs was determined; specific target-cell lysis was calculated as described in Materials and Methods. Data represent mean  $\pm$  SD of triplicate samples. Statistic analysis was performed by using the Student's *T*-test. Data of a representative analysis out of two are shown. **(c,d)** HSPCs express high levels of the granzyme B inactivating PI-9 protease. HSPCs from umbilical cord blood of healthy donors ( $n = 6$ ) were activated for 3 days, stained for PI-9 or with an isotype control antibody (iso) and CD30, respectively. For comparison, peripheral blood lymphocytes of healthy donors ( $n = 4$ ) and cells from lymphoma cell lines ( $n = 3$ ) were stained and analyzed by flow cytometry. **(e)** Comparison of PI-9 expression between HSPC, peripheral blood lymphocytes and lymphoma cell lines, respectively. **(d)** Comparison of PI-9 expression between CD30<sup>+</sup> and CD30<sup>-</sup> HSPC. Data represent mean values  $\pm$  SD where applicable. **(e)** HSPCs upregulate PI-9 upon cytokine-mediated activation. Isolated HSPCs ( $n = 3$ ) were cultivated either without activation or activated for 3 days as described above. Cells were recovered and stained for PI9 and analyzed by flow cytometry. Data represent mean values  $\pm$  SD. Statistical analysis was performed by using the Student's *T*-test and significant differences were indicated.

CAR-mediated T-cell activation requires CAR cross-linking upon antigen engagement in order to form supra-molecular clusters, so-called signaling synapses.<sup>24</sup> The number of accessible CD30 molecules on the cell surface is thereby a key factor for the efficiency in CAR clustering and finally in T-cell activation. By engineering MC38 cells with various levels of CD30, we revealed that there is a ceiling of CD30 dose above which increase in CD30 levels did not furthermore increase cytotoxicity by anti-CD30 CAR T cells. In contrast, induction of IFN- $\gamma$  release by CAR T cells increased above the ceiling density for killing. As a consequence, CD30<sup>low</sup> cells like CD30<sup>+</sup> HSPCs did not evoke a proinflammatory cytokine response and were not substantially lysed while CD30<sup>high</sup> MyLa cells induced cytotoxicity and IFN- $\gamma$  release by CAR T cells.

The data were confirmed utilizing CD30<sup>-</sup> and CD30<sup>+</sup> activated B cells as target cells that also expressed CD30 nearby or below the activation threshold of the anti-CD30 CAR T cells. Moreover, despite some basal degranulation of anti-CD30 CAR T cells that may be due to CD30 expression on activated T cells resulting in "spontaneous" self ligation of the CAR, we observed target cell-specific degranulation of CAR T cells only in presence of CD30<sup>high</sup> lymphoma cells but not CD30<sup>low</sup> HSPC.

Second, HSPCs show increased levels of the PI-9 serine protease which is part of the cell-intrinsic protection machinery towards granzyme-mediated cytotoxicity. The predominant mechanism of cytotoxicity by CAR-activated T cells is based on perforin and granzyme B; Fas/FasL-mediated cell death is of less impact

in this context.<sup>25</sup> Transfer of granzyme into target cells during a cytolytic T-cell attack activates executor caspases and cell death which can be prevented by high levels of the serine protease PI-9/serpin-6 (SP6) that irreversibly inactivates granzyme B.<sup>26</sup> Human CD34<sup>+</sup> HSPCs seem to be protected by such a mechanism since these cells have high PI-9 levels that were further upregulated upon cytokine-mediated activation (cf. **Figure 7c,e**). Similarly, embryonic and mesenchymal stem cells are protected from cytolytic destruction by high levels of PI-9.<sup>18–20</sup>

In the case of an anti-CD30 CAR T-cell therapy, activated CD30<sup>+</sup> HSPCs are protected by sub- or near-threshold CD30 levels for T-cell activation and by high SP-6/PI9 levels. In contrast, lymphoma cells provide high CD30 levels and are efficiently lysed by CAR T cells. These profound differences in the recognition and killing of healthy and malignant cells constitutes a remarkable high therapeutic index of the anti-CD30 CAR T cells making an adoptive therapy of CD30<sup>+</sup> malignancies with anti-CD30 CAR T cells feasible and safe. In more general terms, the data imply that a stem cell-related antigen like CD30, which displays different expression levels by tissue stem cells and malignant cells, may be a clinically safe target as long as the tissue stem cells are protected from a cytolytic T-cell attack by cell-intrinsic mechanisms and/or subthreshold levels of the targeted antigen.

## MATERIALS AND METHODS

**Cell lines and reagents.** HEK293T cells are human embryonic kidney cells that express the SV40 large T antigen.<sup>27</sup> The colon carcinoma cell line Colo320 (ATCC CCL 220.1) was obtained from ATCC, Rockville, MD. The CD30<sup>+</sup> lymphoma line MyLa was kindly provided by Prof. R. Dummer, Zurich. The CD30<sup>+</sup> Hodgkin lymphoma cell lines L1236 and L540cy were described earlier.<sup>28</sup> MC38 is a mouse fibrosarcoma cell line which was transfected to express CD30.<sup>29</sup> All cell lines were cultured in RPMI 1640 medium, 10% (v/v) fetal bovine serum (Life Technologies, Paisly, UK). Anti-CD3 mAb OKT3 was purified from OKT3 hybridoma (ATCC CRL 8001) supernatant by affinity chromatography. The anti-HRS3 idiotypic antibody 9G10 was described earlier.<sup>30</sup> The PE-conjugated F(ab')<sub>2</sub> goat anti-human IgG antibody was purchased from Southern Biotechnology. Details of utilized fluorochrome-conjugated antibodies are listed in **Supplementary Table S1**. Respective fluorochrome-conjugated isotype controls were purchased from BD Biosciences, San Diego, CA. Matched antibody pairs for capture and detection of human IFN- $\gamma$  and murine IL-2 were purchased from BD Biosciences. Recombinant IL-2 was obtained from Endogen, Woburn, MA. Immunofluorescence was analyzed using a FACS-Canto cytometer equipped with the Diva software (Becton Dickinson, Mountain View, CA). The human CD30-Fc fusion protein<sup>31</sup> was purified from supernatants of transfected -chinese hamster ovary (CHO) cells and myeloma cells, respectively, by affinity chromatography on anti-human IgG agarose (Sigma, Deisenhofen, Germany), the anti-HRS3 idiotypic mAb 9G10 was described elsewhere.<sup>30</sup>

**Preparation of human T and B cells.** Peripheral blood lymphocytes were obtained from healthy donors by Ficoll density centrifugation. T cells were activated initially by OKT3 (100 ng/ml) and IL-2 (500 U/ml) and further cultivated in the presence of IL-2 (500 U/ml). B cells were isolated from peripheral blood lymphocytes by magnetic-activated cell sorting utilizing anti-CD19 microbeads (Miltenyi Biotec, Bergisch Gladbach, Germany). B cells were activated in the presence of 50 ng/ml soluble CD40L (Immunotools, Friesoythe, Germany) and 10 ng/ml IL-4 (Miltenyi Biotec). CD19<sup>+</sup> B cells were further flow sorted into CD30<sup>+</sup> and CD30<sup>-</sup> subpopulations.

**CARs.** The engineering of the anti-carcinoembryonic antigen and anti-CD30 CARs with the modified CD28-CD3 $\zeta$  signaling domain and the modified IgG1-CH2/3 extracellular spacer domains<sup>10</sup> as well as the retroviral modification of T cells and generation of MD45 T cells with anti-CD30 CAR were described in detail.<sup>32–34</sup> CAR expression was monitored by flow cytometry.

**Isolation of human UCB-derived HSPCs.** Human UCB was obtained from unrelated donors after informed consent according to the Declaration of Helsinki. Mononuclear cells were isolated by Ficoll density gradient centrifugation (Biocoll Separating Solution, Biochrom, Berlin, Germany) and enriched for CD34<sup>+</sup> cells as previously described.<sup>35</sup> Unless indicated otherwise, cells were cultured at a density of 0.5–1  $\times$  10<sup>5</sup> cells/ml in Iscove's modified Dulbecco's medium (Lonza, Cologne, Germany), 20% (v/v) fetal bovine serum (Biochrom), 100 U/ml penicillin, and 100 U/ml streptomycin (Life Technologies, Darmstadt, Germany) and supplemented with FLT3L, stem cell factor (SCF), and thrombopoietin (TPO) (each at 10 ng/ml) (all Miltenyi Biotec) as previously described.<sup>9</sup>

**Flow cytometry and flow cytometric cell sorting.** For flow cytometric cell sorting, CAR-engineered T cells were stained with fluorochrome-labeled anti-human IgG1 and anti-CD3 antibodies, HSPCs were labeled with anti-CD30 and anti-CD34 antibodies and B cells with anti-CD19 and anti-CD30 antibodies, respectively. CAR<sup>+</sup> T cells and CD30<sup>+</sup> HSPCs and B cells, respectively, were identified and purified by flow sorting on a FACSAria cell sorter (Becton Dickinson). For the analysis of CD30 by HSPC subsets cells, CD34<sup>+</sup> cells were additionally antibody stained for the lineage (lin) markers CD3, CD19, CD56, and CD66b as well as for CD45, CD133, CD45RA, CD38, and CD10 as previously described.<sup>14,36</sup> See **Supplementary Table S1** for antibody details and **Supplementary Figures S1 and S2** for the gating strategy. 7-AAD staining (Beckman Coulter) was used for live/dead cell discrimination. Doublets were discriminated using FSC-A versus FSC-W and SSC-A versus SSC-W gating. Data were analyzed by using the FACSDiva (BD) and FlowJo data analysis software (FlowJo LLC, Ashland, OR). Expression of the granzyme B inactivating serine protease PI-9/Sp6 was monitored by intracellular cell staining utilizing the anti-PI-9 mAb (clone 7D8; AbD Serotec, Oxford, UK) and the Intrashure intracellular staining kit (BD Bioscience) according to the manufacturer's recommendations.

**Activation of CAR T cells.** CAR T cells (0.625  $\times$  10<sup>3</sup>–5  $\times$  10<sup>4</sup> cells/well) were cocultivated for 24–48 hours in 96-well round bottom plates with CD30<sup>+</sup> L1236 or MyLa lymphoma cells or CD30<sup>-</sup> Colo320 tumor cells (each 2.5–5  $\times$  10<sup>4</sup> cells/well). Specific cytotoxicity of CAR T cells against target cells was monitored by an XTT (2,3-Bis-(2-Methoxy-4-Nitro-5-Sulphophenyl)-2H-Tetrazolium-5-Carboxanilide)-based colorimetric assay.<sup>37</sup> Viability of tumor cells was monitored using the "Cell Proliferation Kit II" (Roche Diagnostics, Mannheim, Germany). Values were calculated as means of six wells containing tumor cells only subtracted by the mean background level of wells containing medium only. Nonspecific formation of formazane due to the presence of T cells was determined from triplicate wells containing T cells in the same number as in the corresponding experimental wells. The number of viable tumor cells in experimental wells was calculated as follows: viability (%) = (OD (experimental wells–corresponding number of T cells))/(OD (tumor cells without T cells–medium))  $\times$  100. Cytotoxicity (%) was defined as 100–viability (%). Alternatively, MyLa cells were labeled for 5 minutes at 4 °C with 1.25  $\mu$ mol/l CFSE (Molecular Probes, Life Technologies, Darmstadt, Germany), extensively washed and cocultivated in 96-round-bottom plates (2.5  $\times$  10<sup>4</sup> cells/well) with CAR T cells (2.5  $\times$  10<sup>4</sup>/well). After 24–48 hours, cells were recovered, stained with 7-AAD (0.5  $\mu$ g/ml), analyzed by flow cytometry, and the number of live and dead cells was determined. CAR-mediated specific lysis was calculated as follows: specific lysis (%) = (7-AAD<sup>+</sup> target cells in experimental wells (%) – 7-AAD<sup>+</sup> target cells without T cells (%)). Specific lysis of HSPC and B cells, respectively, (1–2  $\times$  10<sup>4</sup>/well) was determined by cocultivation with CAR T cells (2.5  $\times$  10<sup>4</sup>/well) in 96-well round-bottom plates for 24–48 hours. Cells were recovered, stained with 7-AAD and anti-CD34 and anti-CD19 antibodies,

respectively. The numbers of live and dead CD34<sup>+</sup> and CD19<sup>+</sup> cells, respectively, were counted and specific lysis was determined as described above. In some analyses, both HSPCs (10<sup>4</sup> cells/well) and CFSE-labeled MyLa tumor cells (2 × 10<sup>4</sup>/well) were together cocultivated with CAR T cells. Cells were recovered after 24 hours, stained with anti-CD34 mAbs and 7-AAD, and specific lysis was determined by flow cytometry as described above. IFN- $\gamma$  and murine IL2 in culture supernatants was monitored by Enzyme Linked Immunosorbent Assay (ELISA) by binding to the solid-phase anti-IFN- $\gamma$  and IL-2 capture antibody (each 1  $\mu$ g/ml), respectively, and detection by the biotinylated anti-IFN- $\gamma$  or anti-IL-2 detection antibody (0.5  $\mu$ g/ml). The reaction product was visualized by a peroxidase-streptavidin-conjugate (1:10,000) and ABTS (Roche Diagnostics). Blocking of the anti-CD30-CAR by soluble CD30 was tested by coinubation with MD45 anti-CD30-CAR T cells and L540cy cells (each 5 × 10<sup>4</sup>/well) in presence of increasing amounts of sCD30-Fc, the anti-idiotypic mAb 9G10, and an isotype control mAb, respectively. IL-2 secretion was determined by ELISA and percent inhibition of T-cell activation was calculated as follows: inhibition (%) = (mIL-2 release with competitor/mIL-2 release without competitor) × 100.

**Colony-forming cell assay.** For colony-forming cell assays, 200 CD34<sup>+</sup> cells were initially cultivated for 2 days in Iscove's modified Dulbecco's medium supplemented with 20% (v/v) fetal bovine serum and FLT3L, SCF, and TPO (each at 10 ng/ml) in round-bottom 96-well plates. Thereafter culture medium was replaced by RPMI 1640, 10% (v/v) fetal bovine serum for another 24 hours either in the presence or absence of 200 CAR<sup>+</sup> or 200 CAR<sup>-</sup> T cells. Cells were harvested and seeded into 1 ml MethoCult H4434 medium (StemCell Technologies, Cologne, Germany). Hematopoietic colonies were scored after 12–14 days as previously described.<sup>14,36</sup>

**Degranulation assay.** For recording of cytotoxic granule exocytosis, 2.5 × 10<sup>4</sup> CAR T cells and 2.5 × 10<sup>4</sup> target cells (MyLa, HSPC) were cocultivated for 12 hours in the presence of monensin (2  $\mu$ mol/l, Abcam, Cambridge, UK) and the fluorescein isothiocyanate (FITC)-conjugated anti-CD107a mAb. Cells were recovered stained with anti-CD3-APC and anti-human IgG1-Fc-PE antibodies, analyzed by flow cytometry and the number of CD3<sup>+</sup>CAR<sup>+</sup>CD107a<sup>+</sup> cells was determined.

**CAR T cell-mediated suppression of tumor growth.** Rag2<sup>-/-</sup>  $\gamma$ C<sup>-/-</sup> mice (Charles River, Sulzfeld, Germany) (five or six animals/group) were subcutaneously inoculated with MyLa lymphoma (10<sup>7</sup> cells/animal) and CAR T cells (2.5 × 10<sup>5</sup>–10<sup>7</sup> cells/animal). T cells without CAR served as control. Tumor volumes were recorded every 2–3 days. Area under curve was recorded as described<sup>38</sup>, and statistical analyses were performed by the Student's *T*-test.

**Engraftment of HSPCs in immune-deficient mice.** Newborn Rag2<sup>-/-</sup>  $\gamma$ C<sup>-/-</sup> mice were irradiated twice with 2 Gray X-ray each in a three to four hour interval. Four to six hours after the second irradiation, mice were intrahepatically transplanted with UCB HSPCs (1–3 × 10<sup>5</sup> CD34<sup>+</sup> cells/mouse). After 5–6 weeks, successful engraftment was confirmed by the detection of human CD4<sup>+</sup>CD45<sup>+</sup> T cells in the peripheral blood of the transplanted mice; nontransplanted animals served as control. Autologous T cells from the same donor were engineered with the CAR as described above and cells were intravenously applied (2.5 × 10<sup>6</sup> CAR T cells/mouse). The numbers of human CD30<sup>+</sup>CD4<sup>+</sup> T and CD30<sup>+</sup>CD19<sup>+</sup> B cells in the peripheral blood of mice were recorded by flow cytometry.

**Statistics.** Experimental results from independent representative experiments are reported as mean values ± standard deviation. Significance was calculated by the two-sided Student's *T*-test using Microsoft Excel and Graphpad Prism, respectively.

## SUPPLEMENTARY MATERIAL

**Figure S1.** Gating strategy to identify subsets of HSPCs.

**Figure S2.** PCR Detection of the CAR in tissues of CAR T cell engrafted huSCID mice.

**Table S1.** Monoclonal antibodies utilized for this study.

## ACKNOWLEDGMENTS

We thank Angela Köninger and Rainer Kimmig (Gynecology Department, University Hospital Essen, Essen, Germany) for providing umbilical cord blood samples. Work in the H.A. laboratory was supported by grants from the Deutsche Forschungsgemeinschaft, Bonn, the Deutsche Krebshilfe, Bonn, and the Deutsche José Carreras Leukämie-Stiftung, München, Germany.

## REFERENCES

- Porter, DL, Levine, BL, Kalos, M, Bagg, A and June, CH (2011). Chimeric antigen receptor-modified T cells in chronic lymphoid leukemia. *N Engl J Med* **365**: 725–733.
- Grupp, SA, Kalos, M, Barrett, D, Aplenc, R, Porter, DL, Rheingold, SR *et al.* (2013). Chimeric antigen receptor-modified T cells for acute lymphoid leukemia. *N Engl J Med* **368**: 1509–1518.
- Nakamura, T, Lee, RK, Nam, SY, Al-Ramadi, BK, Koni, PA, Bottomly, K *et al.* (1997). Reciprocal regulation of CD30 expression on CD4<sup>+</sup> T cells by IL-4 and IFN- $\gamma$ . *J Immunol* **158**: 2090–2098.
- Muta, H and Podack, ER (2013). CD30: from basic research to cancer therapy. *Immunol Res* **57**: 151–158.
- Kumar, A and Younes, A (2014). Role of CD30 targeting in malignant lymphoma. *Curr Treat Options Oncol* **15**: 210–225.
- Hombach, A, Heuser, C, Sircar, R, Tillmann, T, Diehl, V, Pohl, C *et al.* (1998). An anti-CD30 chimeric receptor that mediates CD3-zeta-independent T-cell activation against Hodgkin's lymphoma cells in the presence of soluble CD30. *Cancer Res* **58**: 1116–1119.
- Savoldo, B, Rooney, CM, Di Stasi, A, Abken, H, Hombach, A, Foster, AE *et al.* (2007). Epstein Barr virus specific cytotoxic T lymphocytes expressing the anti-CD30zeta artificial chimeric T-cell receptor for immunotherapy of Hodgkin disease. *Blood* **110**: 2620–2630.
- Hombach, A, Muche, JM, Gerken, M, Gellrich, S, Heuser, C, Pohl, C *et al.* (2001). T cells engrafted with a recombinant anti-CD30 receptor target autologous CD30(+) cutaneous lymphoma cells. *Gene Ther* **8**: 891–895.
- Beckmann, J, Scheitza, S, Wernet, P, Fischer, JC and Giebel, B (2007). Asymmetric cell division within the human hematopoietic stem and progenitor cell compartment: identification of asymmetrically segregating proteins. *Blood* **109**: 5494–5501.
- Hombach, A, Hombach, AA and Abken, H (2010). Adoptive immunotherapy with genetically engineered T cells: modification of the IgG1 Fc 'spacer' domain in the extracellular moiety of chimeric antigen receptors avoids 'off-target' activation and unintended initiation of an innate immune response. *Gene Ther* **17**: 1206–1213.
- Kofler, DM, Chmielewski, M, Rapp, G, Hombach, A, Riet, T, Schmidt, A *et al.* (2011). CD28 costimulation impairs the efficacy of a redirected T-cell antitumor attack in the presence of regulatory T cells which can be overcome by preventing Lck activation. *Mol Ther* **19**: 760–767.
- Zanotti, R, Trolese, A, Ambrosetti, A, Nadali, G, Visco, C, Ricetti, MM *et al.* (2002). Serum levels of soluble CD30 improve International Prognostic Score in predicting the outcome of advanced Hodgkin's lymphoma. *Ann Oncol* **13**: 1908–1914.
- Horie, R and Watanabe, T (1998). CD30: expression and function in health and disease. *Semin Immunol* **10**: 457–470.
- Görgens, A, Radtke, S, Möllmann, M, Cross, M, Dürig, J, Horn, PA *et al.* (2013). Revision of the human hematopoietic tree: granulocyte subtypes derive from distinct hematopoietic lineages. *Cell Rep* **3**: 1539–1552.
- Radtke, S, Görgens, A, Kordelas, L, Schmidt, M, Kimmig, KR, Köninger, A *et al.* (2015). CD133 allows elaborated discrimination and quantification of haematopoietic progenitor subsets in human haematopoietic stem cell transplants. *Br J Haematol* **169**: 868–878.
- de Bruin, PC, Gruss, HJ, van der Valk, P, Willemse, R and Meijer, CJ (1995). CD30 expression in normal and neoplastic lymphoid tissue: biological aspects and clinical implications. *Leukemia* **9**: 1620–1627.
- Sun, J, Bird, CH, Sutton, V, McDonald, L, Coughlin, PB, De Jong, TA *et al.* (1996). A cytosolic granzyme B inhibitor related to the viral apoptotic regulator cytokine response modifier A is present in cytotoxic lymphocytes. *J Biol Chem* **271**: 27802–27809.
- El Haddad, N, Moore, R, Heathcote, D, Mounayar, M, Azzi, J, Mfarrej, B *et al.* (2011). The novel role of SERPINB9 in cytotoxic protection of human mesenchymal stem cells. *J Immunol* **187**: 2252–2260.
- El Haddad, N, Heathcote, D, Moore, R, Yang, S, Azzi, J, Mfarrej, B *et al.* (2011). Mesenchymal stem cells express serine protease inhibitor to evade the host immune response. *Blood* **117**: 1176–1183.
- Utermöhlen, O and Krönke, M (2007). Survival of priceless cells: active and passive protection of embryonic stem cells against immune destruction. *Arch Biochem Biophys* **462**: 273–277.
- Doti, G, Gottschalk, S, Savoldo, B and Brenner, MK (2014). Design and development of therapies using chimeric antigen receptor-expressing T cells. *Immunol Rev* **257**: 107–126.
- Grupp, SA, Kalos, M, Barrett, D, Aplenc, R, Porter, DL, Rheingold, SR *et al.* (2013). Chimeric antigen receptor-modified T cells for acute lymphoid leukemia. *N Engl J Med* **368**: 1509–1518.
- Lee, DW, Kochenderfer, JN, Stetler-Stevenson, M, Cui, YK, Delbrook, C, Feldman, SA *et al.* (2015). T cells expressing CD19 chimeric antigen receptors for acute lymphoblastic leukaemia in children and young adults: a phase 1 dose-escalation trial. *Lancet* **385**: 517–528.
- Rapp, G, Riet, T, Awerkwiew, S, Schmidt, M, Hombach, AA, Pfister, H *et al.* (2012). The CD3-zeta chimeric antigen receptor overcomes TCR Hypo-responsiveness of human terminal late-stage T cells. *PLoS One* **7**: e30713.
- Hombach, A, Köhler, H, Rapp, G and Abken, H (2006). Human CD4<sup>+</sup> T cells lyse target cells via granzyme/perforin upon circumvention of MHC class II restriction by an antibody-like immunoreceptor. *J Immunol* **177**: 5668–5675.

26. Kaiserman, D and Bird, PI (2010). Control of granzymes by serpins. *Cell Death Differ* **17**: 586–595.
27. Graham, FL, Smiley, J, Russell, WC and Nairn, R (1977). Characteristics of a human cell line transformed by DNA from human adenovirus type 5. *J Gen Virol* **36**: 59–74.
28. Wolf, J, Kapp, U, Bohlen, H, Kornacker, M, Schoch, C, Stahl, B *et al.* (1996). Peripheral blood mononuclear cells of a patient with advanced Hodgkin's lymphoma give rise to permanently growing Hodgkin-Reed Sternberg cells. *Blood* **87**: 3418–3428.
29. Schwegler, C, Dorn-Beineke, A, Nittka, S, Stocking, C and Neumaier, M (2005). Monoclonal anti-idiotype antibody 6G6.C4 fused to GM-CSF is capable of breaking tolerance to carcinoembryonic antigen (CEA) in CEA-transgenic mice. *Cancer Res* **65**: 1925–1933.
30. Pohl, C, Renner, C, Schwonzen, M, Schobert, I, Liebenberg, V, Jung, W *et al.* (1993). CD30-specific AB1-AB2-AB3 internal image antibody network: potential use as anti-idiotype vaccine against Hodgkin's lymphoma. *Int J Cancer* **54**: 418–425.
31. Renner, C, Jung, W, Sahin, U, van Lier, R and Pfreundschuh, M (1995). The role of lymphocyte subsets and adhesion molecules in T cell-dependent cytotoxicity mediated by CD3 and CD28 bispecific monoclonal antibodies. *Eur J Immunol* **25**: 2027–2033.
32. Weijtens, ME, Willemsen, RA, Hart, EH and Bolhuis, RL (1998). A retroviral vector system 'STITCH' in combination with an optimized single chain antibody chimeric receptor gene structure allows efficient gene transduction and expression in human T lymphocytes. *Gene Ther* **5**: 1195–1203.
33. Hombach, A, Wieczarkowicz, A, Marquardt, T, Heuser, C, Usai, L, Pohl, C *et al.* (2001). Tumor-specific T cell activation by recombinant immunoreceptors: CD3 zeta signaling and CD28 costimulation are simultaneously required for efficient IL-2 secretion and can be integrated into one combined CD28/CD3 zeta signaling receptor molecule. *J Immunol* **167**: 6123–6131.
34. Hombach, A, Heuser, C, Gerken, M, Fischer, B, Lewalter, K, Diehl, V *et al.* (2000). T cell activation by recombinant FcepsilonRI gamma-chain immune receptors: an extracellular spacer domain impairs antigen-dependent T cell activation but not antigen recognition. *Gene Ther* **7**: 1067–1075.
35. Giebel, B, Corbeil, D, Beckmann, J, Höhn, J, Freund, D, Giesen, K *et al.* (2004). Segregation of lipid raft markers including CD133 in polarized human hematopoietic stem and progenitor cells. *Blood* **104**: 2332–2338.
36. Görgens, A, Ludwig, AK, Möllmann, M, Krawczyk, A, Dürig, J, Hanenberg, H *et al.* (2014). Multipotent hematopoietic progenitors divide asymmetrically to create progenitors of the lymphomyeloid and erythromyeloid lineages. *Stem Cell Reports* **3**: 1058–1072.
37. Jost, LM, Kirkwood, JM and Whiteside, TL (1992). Improved short- and long-term XTT-based colorimetric cellular cytotoxicity assay for melanoma and other tumor cells. *J Immunol Methods* **147**: 153–165.
38. Duan, F, Simeone, S, Wu, R, Grady, J, Mandouli, I and Srivastava, PK (2012). Area under the curve as a tool to measure kinetics of tumor growth in experimental animals. *J Immunol Methods* **382**: 224–228.